Structural Memory in Pressure-Amorphized $AlPO_4$

John S. Tse and Dennis D. Klug

Molecular dynamics simulations reveal the mechanism of the structural memory effect in α-berlinite ($AlPO_4$), where a single crystal transforms to an amorphous solid by compression and then reverts to the original crystalline structure upon release of pressure. The enhanced oxygen coordination around the aluminum atoms in $AlPO_4$ at high pressure leads to a mechanical instability that causes the phase transformation. The difference in the structural memory behavior between $AlPO_4$ and isostructural α-quartz, for which the pressure-induced amorphized phase is recoverable, can be attributed to the presence of the PO_4 units, which remain essentially four-coordinated even when severely distorted.

THE TRADITIONAL VIEW OF GLASS structure is that both short-range and long-range order are absent and the structure is best described as a continuous random network (*1, 2*). Recently, it has been reported that in some glasses the local ordering prevails over an intermediate range of several atomic or molecular units (*3*). This finding raised the basic question of the extent to which amorphous solids are disordered. The loss of long-range order is often identified by the growth of diffuse scattering in the diffraction pattern (*4*). However, it is often difficult to characterize the short-range structure.

It was recently suggested that, if a crystalline solid is compressed beyond its extrapolated melting line, it may transform into a quenchable disordered solid with a structure resembling that of a liquid (*5*). This suggestion has been tested in several materials (*6*). Two interesting and puzzling cases are those of the isostructural materials α-quartz and α-berlinite ($AlPO_4$) (*7*). At room temperature, α-quartz transforms into a high-density phase at 20 to 30 GPa that is recoverable at ambient pressure. The diffraction pattern indicates that the high-pressure phase is disordered. In contrast, crystalline $AlPO_4$ undergoes a similar densification at 18 GPa, but the transformation is reversible. It is more remarkable that, when the experiment was performed on a single crystal, both the crystal structure and orientation were recovered (*7*). Apparently, the disordered $AlPO_4$ retained a structural memory of the crystalline state. The contrasting behavior of these two systems indicates that there must be a large range of types of disorder among pressure-amorphized solids. The reversible transformation of the pressure-amorphized phases to the starting crystalline solids has also been observed in SnI_4, $LiKSO_4$, $Ca(OH)_2$, clathrate hydrates, and clathrasils (*8*).

Molecular dynamics (MD) investigations of the static and dynamical properties of several phases of silica have shown that recently proposed two-body potentials can be used to accurately describe these materials (*9*). For pressure-induced amorphization of α-quartz, the MD calculations not only correctly reproduce the experimental transition but also offer information concerning the detailed mechanism. The analysis of the theoretical results indicated that a mechanical instability causes the transition from α-quartz to a disordered solid (*10*). The increased interactions between the Si atoms and their adjacent oxygen atoms due to the tilting and distortion of the SiO_4 tetrahedra is the primary energetic reason for the transformation. The MD calculations not only corroborated the suggestion derived from more sophisticated first-principles electronic structure calculations (*11*), they also offered more detailed information on the mechanism at the atomic level.

To examine the mechanism in $AlPO_4$, we carried out isothermal-isobaric MD simulations. This method allows both the volume and the shape of the MD cell to change in response to external perturbations (*12*). We used the two-body potential proposed by van Beest *et al.* (*13*), which was constructed in the same manner as that used successfully for the investigation of the pressure-induced amorphization of α-quartz (*10*). The model system consisted of 96 formula units with initial atomic positions taken from the x-ray structure at ambient pressure (*14*). Time steps of 1 to 1.5 fs were used in the integration of the equations of motion. At each pressure, the system was equilibrated at 300 K for about 5000 time steps. The calculated equilibrium properties were averaged for at least 3 ps.

The calculated volume and energy of $AlPO_4$ as a function of pressure (Fig. 1) and the *c/a* ratio are in good agreement with the available experimental results at low pressure (*14*). Below 31 GPa, $AlPO_4$ compresses elastically. The observed volume discontinuity of about 4% and a small change in the slope of the curve of energy versus pressure at 31 GPa indicate a phase transition. Both the volume and energy changes accompanying this transformation are small compared to those accompanying the transformation in quartz. After the pressure was increased to 80 GPa, it was lowered gradually in steps to 1 bar. The calculated x-ray patterns after the transition is characteristic of a disordered material. The diffraction patterns of the starting material and of the recovered sample at 1 bar, however, were essentially identical. This similarity indicates that the transformation is reversible.

Comparison of the instantaneous structures of the original, transformed, and recovered sample (Fig. 2) clearly shows that both the crystal structure and the orientation are recovered upon decompression and that the high-pressure phase is disordered. The calculated atomic vibrational density of the crystalline and the transformed phases at 1 bar and 40 GPa, respectively, show that, although the P–O stretching modes at 1000 cm^{-1} are preserved, the predominantly Al–O stretching band at 800 cm^{-1} has greatly broadened in the disordered phase. The theoretical results are in complete agreement with the x-ray diffraction and infrared measurements (7). The transition pressure is predicted to be somewhat higher, however,

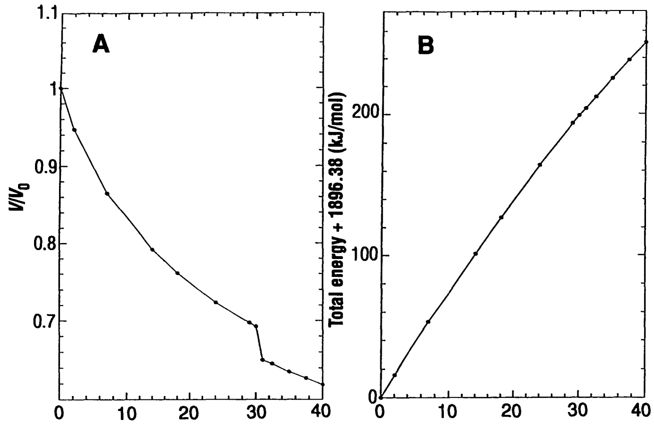

Fig. 1. The calculated molar volume (**A**) and energy (**B**) versus pressure at 300 K.

Steacie Institute for Molecular Sciences, National Research Council of Canada, Ottawa, Ontario, Canada K1A 0R6.

perhaps because of incomplete optimization of the potential. It is unlikely that the calculated reversible transformation is an artifact of the system size. The same number of atoms was used in an earlier calculation on the pressure amorphization of α-quartz (*10*). The contrasting behavior of the two systems must therefore be due to the intrinsic differences in the atomic interactions.

In order to obtain a full understanding of the pressure-induced reversible order-disorder transformation in $AlPO_4$, a more detailed analysis is required. The pretransition structural changes of $AlPO_4$ and isostructural α-quartz are similar. Upon compression, the spiraling AlO_4 and PO_4 tetrahedra distort and rotate into the empty space in the lattice, thus increasing the interaction between the Al and their next-nearest neighbor oxygens. The O–P–O and O–Al–O angle distributions calculated as a function of pressure (Fig. 3) are in good agreement with recent low-pressure experimental results (*14*). The average O–P–O and O–Al–O angles at 1 bar are close to the tetrahedral angles. As pressure increases, both angular distributions split and deviate from 109.5° with the O–Al–O distribution somewhat broader than the O–P–O distribution. The distortion of the valence angles is a consequence of the twisting and flattening of the tetrahedra. Immediately after the transition at 31 GPa, the O–Al–O angle distribution broadens significantly and peaks around 96°. This change is accompanied by an abrupt increase in the average oxygen coordination to 5 and then gradually to 6 by 40 GPa. In contrast, the O–P–O angles are distributed almost evenly around 108° as if the PO_4 units have nearly remained as tetrahedra.

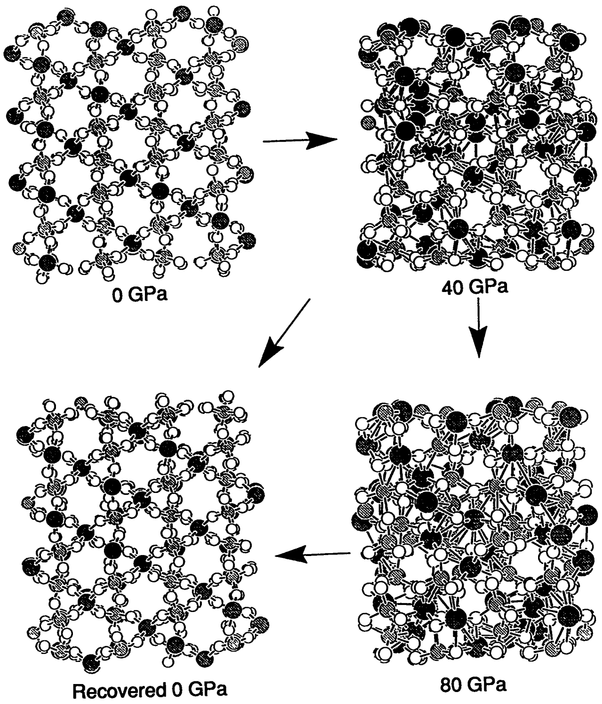

Fig. 2. The calculated structure of the $AlPO_4$ sample viewed down the *c* axis at 1 bar, 40 GPa, 80 GPa, and after releasing the pressure to 1 bar. The black balls are Al atoms, the gray balls are P atoms, and the white balls are O atoms.

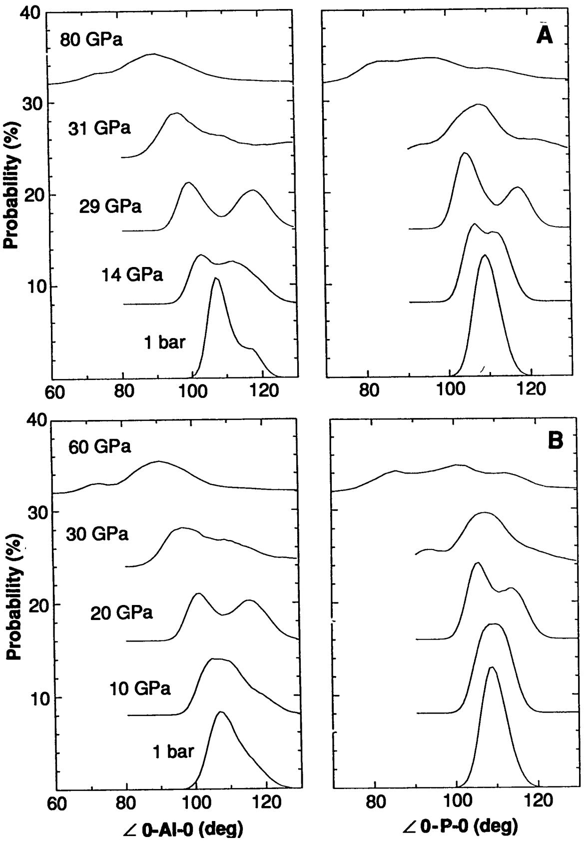

Fig. 3. The calculated distribution of O–Al–O and O–P–O angles upon raising (**A**) and lowering (**B**) the pressure on $AlPO_4$.

The Al–O and P–O nearest-neighbor distances show little change with pressure. On the other hand, the Al–P distances decrease as the Al–O–P angles decrease, and the next-nearest neighbor Al–O and P–O distances decrease gradually with pressure from about 3.8 Å at ambient pressure to about 2.9 Å just before the transition. At 80 GPa, the distortion of the PO_4 local structure becomes more severe, with the average oxygen coordination increasing slightly to 4.6. This observation is in good agreement with the results of a Raman study (*15*). Therefore, under pressure, a PO_4 unit from a neighboring spiral is tilted and forced into an interstitial site near the Al atom, and an O atom on a connected PO_4 unit enters the coordination sphere of the Al atom (Fig. 4). The highly repulsive interactions due to the crowding of the atoms induce a mechanical instability that is compensated by the energy gained from the formation of new Al–O bonds after the phase transition with little change in the PO_4 local structure. This suggestion is supported by the observation that it is common to find AlO_6 units in crystal structures, but PO_n units with $n > 4$ are rare. The preservation of the P–O coordination in $AlPO_4$ also limits the volume change at the order-disorder transition to only one-fourth of that calculated for α-quartz. Although the transformation is displacive in nature, there is no substantial rearrangement of the local structure.

The pressure was then released from 80 GPa in steps of 10 GPa. A snapshot of the recovered phase (Fig. 2) shows that not only

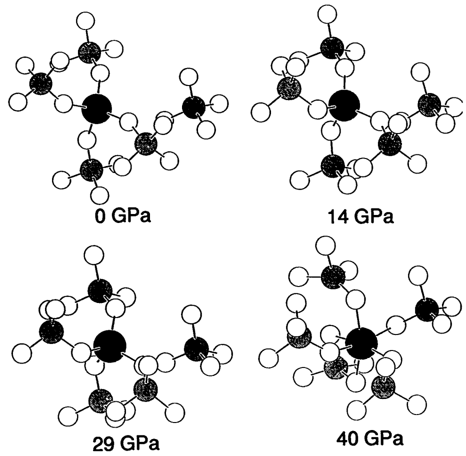

Fig. 4. The local structure about a typical Al atom in $AlPO_4$ at several pressures. The coordination number of an aluminum atom is indicated by the lines to oxygen atoms corresponding to lengths of 2.2 Å or less.

is the crystallinity of the sample fully restored, but its original orientation is also preserved. Details of the recovery mechanism can be examined through the analysis of bond angles, as presented above. The path following decompression retraces that of the compression (Fig. 3). Both the O–Al–O and the O–P–O angle distributions narrow and eventually return to tetrahedral angles in such a way that the tetrahedral helices unwind to their original positions. The PO_4 groups, which alternate with AlO_4 groups in the crystal, distort under pressure but remain largely four-coordinated. In the absence of diffusion, the relative positions of the atoms are effectively maintained in the disordered phase. When the pressure releases, the oxygens around the P atoms quickly relax back to the PO_4 tetrahedra. This process redirects the Al atoms back to the crystalline positions.

Several significant observations can be made from the theoretical investigation. The pressure-induced densified phase in $AlPO_4$ is not a random network but a solid that is disordered over the long range with considerable short-range order. Because of the lack of diffusion, pressure-amorphized materials would not, in general, have the same structure as quenched liquids. Attempts to correlate the structure of the disordered solid to that of high-density liquid may be misleading. The results obtained here can be generalized to other systems that exhibit structural memory effects. The presence of strongly covalently bound units that preserve their coordinations is essential, as, for example, the SO_4^{2-} in $LiKSO_4$ and the guest molecules in clathrate hydrates and clathrasils. In clathrate hydrates or clathrasils (*8*), the guest molecules remains intact, and therefore their pressure-induced phase transitions are reversible. This behavior is in contrast to that observed in closely related materials, ice Ih (*5*) and α-quartz (*6*).

REFERENCES AND NOTES

1. Y. Waseda, *Structure of Non-Crystalline Materials: Liquids and Amorphous Solids* (McGraw-Hill, New York, 1980); S. R. Elliot, *Physics of Amorphous Materials* (Wiley, New York, ed. 2, 1990).
2. W. H. Zachariasen, *J. Am. Chem. Soc.* **54**, 3841 (1932); R. Zallen, *The Physics of Amorphous Solids* (Wiley, New York, 1983).
3. I. Amato, *Science* **252**, 1377 (1991); P. Gaskell, M. C. Eckersley, A. C. Barnes, P. Chieux, *Nature* **350**, 675 (1991).
4. B. E. Warren, *X-Ray Diffraction* (Addison-Wesley, Reading, MA, 1969).
5. O. Mishima, L. D. Calvert, E. Whalley, *Nature* **310**, 393 (1984); E. Whalley, O. Mishima, Y. P. Handa, D. D. Klug, *Ann. N.Y. Acad. Sci.* **484**, 81 (1986); J. S. Tse and M. L. Klein, *Phys. Rev. Lett.* **58**, 1672 (1987).
6. R. J. Hemley, A. P. Jephcoat, H. K. Mao, L. C. Ming, M. H. Manghnani, *Nature* **334**, 52 (1988).
7. A. Jayaraman, D. L. Wood, R. G. Mains, Sr., *Phys. Rev. B* **35**, 8316 (1987); M. B. Kruger and R. Jeanloz, *Science* **249**, 647 (1990).
8. Y. Fujii *et al.*, *J. Phys. C* **18**, 789 (1985); S. Sugai, *ibid.*, p. 799; H. Sankaran *et al.*, *Phys. Rev. B* **38**, 170 (1988); M. B. Kruger *et al.*, *J. Chem. Phys.* **91**, 5910 (1989); Y. P. Handa, J. S. Tse, D. D. Klug, E. Whalley, *ibid.* **94**, 623 (1991); J. S. Tse, D. D. Klug, J. A. Ripmeester, in preparation.
9. J. S. Tse and D. D. Klug, *J. Chem. Phys.* **95**, 9176 (1991); S. Tsuneyuki, M. Tsukada, H. Aoki, Y. Matsui, *Phys. Rev. Lett.* **61**, 869 (1988).
10. J. S. Tse and D. D. Klug, *Phys. Rev. Lett.* **67**, 3559 (1991).
11. J. R. Chelikowsky, H. E. King, Jr., N. Troullier, J. L. Martins, J. Glinnemann, *ibid.* **65**, 3309 (1990); J. R. Chelikowsky, H. E. King, Jr., J. Glinnemann, *Phys. Rev. B* **15**, 10866 (1990).
12. S. Nosé, *J. Chem. Phys.* **81**, 511 (1984); ——— and M. L. Klein, *Mol. Phys.* **50**, 1055 (1983).
13. B. W. H. van Beest, G. J. Kramer, R. A. van Santen, *Phys. Rev. Lett.* **64**, 1955 (1990).
14. H. Sowa, J. Macavei, H. Schulz, *Z. Kristallogr.* **192**, 119 (1990).
15. M. B. Kruger and R. Jeanloz, *Eos* **70**, 1385 (1990).

27 November 1991; accepted 23 January 1992

Bulk Chemical Characteristics of Dissolved Organic Matter in the Ocean

RONALD BENNER,* J. DEAN PAKULSKI, MATTHEW MCCARTHY, JOHN I. HEDGES, PATRICK G. HATCHER

Dissolved organic matter (DOM) is the largest reservoir of reduced carbon in the oceans. The nature of DOM is poorly understood, in part, because it has been difficult to isolate sufficient amounts of representative material for analysis. Tangential-flow ultrafiltration was shown to recover milligram amounts of >1000 daltons of DOM from seawater collected at three depths in the North Pacific Ocean. These isolates represented 22 to 33 percent of the total DOM and included essentially all colloidal material. The elemental, carbohydrate, and carbon-type (by ^{13}C nuclear magnetic resonance) compositions of the isolates indicated that the relative abundance of polysaccharides was high (~50 percent) in surface water and decreased to ~25 percent in deeper samples. Polysaccharides thus appear to be more abundant and reactive components of seawater DOM than has been recognized.

DISSOLVED ORGANIC MATTER (DOM) in the oceans is important in the global carbon cycle (*1*), supports heterotrophic activity (*2*), and affects the penetration of light and exchange of gases at the sea surface (*3*). Despite its importance, relatively little is known about the composition and reactivity of marine DOM because of the lack of suitable methods for its isolation from seawater. Direct biochemical analyses of DOM in seawater typically account for less than 15% of the total mixture (*4*, *5*), and many techniques that would provide more comprehensive structural information, such as nuclear magnetic resonance (NMR) and infrared spectroscopy, require the isolation of DOM from the much more abundant salts in seawater. The conventional method for isolation has been adsorption of acidified DOM onto nonionic XAD resins (*6*). However, this method typically recovers a small fraction (5 to 15%) of the total DOM in seawater, requires large manipulations of pH during isolation, and is selective for hydrophobic constituents.

In contrast, tangential-flow ultrafiltration concentrates organic molecules primarily on the basis of size rather than chemical properties (*7*) and requires no pH adjustments that may change chemical associations and structures. Ultrafiltration therefore appears to be a more appropriate method for isolating a representative fraction of DOM than adsorption on XAD resins. In this report we describe the

---

R. Benner and J. D. Pakulski, Marine Science Institute, University of Texas at Austin, Port Aransas, TX 78373.
M. McCarthy and J. I. Hedges, School of Oceanography, University of Washington, Seattle, WA 98195.
P. G. Hatcher, Fuel Science Program, The Pennsylvania State University, University Park, PA 16802.

*To whom correspondence should be addressed.